

See discussions, stats, and author profiles for this publication at: <https://www.researchgate.net/publication/259880580>

# How Solvent Influences the Anomeric Effect: Roles of Hyperconjugative versus Steric Interactions on the Conformational Preference

ARTICLE *in* THE JOURNAL OF ORGANIC CHEMISTRY · JANUARY 2014

Impact Factor: 4.72 · DOI: 10.1021/jo402306e · Source: PubMed

CITATIONS

3

READS

47

4 AUTHORS, INCLUDING:



**Changwei Wang**

China University of Petroleum

11 PUBLICATIONS 75 CITATIONS

SEE PROFILE



**Wei Wu**

Xiamen University

102 PUBLICATIONS 2,032 CITATIONS

SEE PROFILE



**Yirong Mo**

Western Michigan University

140 PUBLICATIONS 3,717 CITATIONS

SEE PROFILE

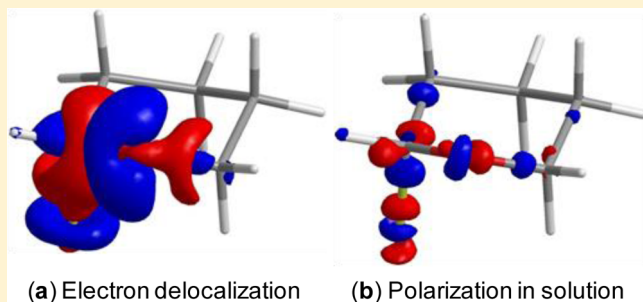
# How Solvent Influences the Anomeric Effect: Roles of Hyperconjugative versus Steric Interactions on the Conformational Preference

Changwei Wang,<sup>†,‡</sup> Fuming Ying,<sup>†</sup> Wei Wu,<sup>\*,†</sup> and Yirong Mo<sup>\*,‡</sup>

<sup>†</sup>The State Key Laboratory of Physical Chemistry of Solid Surfaces, Fujian Provincial Key Laboratory of Theoretical and Computational Chemistry, and College of Chemistry and Chemical Engineering, Xiamen University, Xiamen, Fujian 361005, China

<sup>‡</sup>Department of Chemistry, Western Michigan University, Kalamazoo, Michigan 49008, United States

**ABSTRACT:** The block-localized wave function (BLW) method, which can derive optimal electron-localized state with intramolecular electron delocalization completely deactivated, has been combined with the polarizable continuum model (PCM) to probe the variation of the anomeric effect in solution. Currently both the hyperconjugation and electrostatic models have been called to interpret the anomeric effect in carbohydrate molecules. Here we employed the BLW-PCM scheme to analyze the energy differences between  $\alpha$  and  $\beta$  anomers of substituted tetrahydropyran  $C_5OH_2Y$  ( $Y = F, Cl, OH, NH_2$ , and  $CH_3$ ) and tetrahydrothiopyran  $C_5SH_2Y$  ( $Y = F, Cl, OH$ , and  $CH_3$ ) in solvents including chloroform, acetone, and water. In accord with literature, our computations show that for anomeric systems the conformational preference is reduced in solution and the magnitude of reduction increases as the solvent polarity increases. Significantly, on one hand the solute–solvent interaction diminishes the intramolecular electron delocalization in  $\beta$  anomers more than in  $\alpha$  anomers, thus destabilizing  $\beta$  anomers relatively. But on the other hand, it reduces the steric effect in  $\beta$  anomers much more than  $\alpha$  anomers and thus stabilizes  $\beta$  anomers relatively more, leading to the overall reduction of the anomeric effect in anomeric systems in solutions.

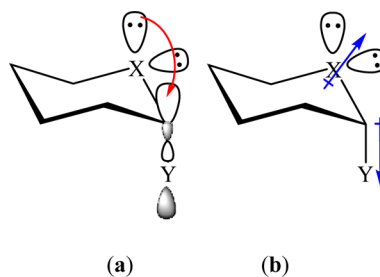


## INTRODUCTION

The anomeric effect is a celebrated phenomenon in carbohydrate chemistry, and the term is designated for the thermodynamic preference of an electronegative substituent ( $Y$ ) at the anomeric carbon center adjacent to the endocyclic oxygen atom in a glycopyranosyl derivative to adopt an axial position ( $\alpha$  anomer) rather than an equatorial position ( $\beta$  anomer) in the chair conformation.<sup>1–3</sup> This is in contrast to the prediction based on conventional steric interactions that the less crowded  $\beta$  anomers would be favored over  $\alpha$  anomers, as exemplified by substituted cyclohexanes. While the anomeric effect ubiquitously exists in monosaccharides and their derivatives, this stereoelectronic effect has now been recognized in saturated heterocycles and acyclic systems containing heteroatoms ( $X = O, N, S$ , and  $P$ ).<sup>4–9</sup> Compared with the corresponding  $\beta$  anomer,  $\alpha$  anomer involves a shortened (strengthened)  $C-X$  bond and a lengthened (weakened)  $C-Y$  bond in a  $R-X-C-Y$  moiety.<sup>10–17</sup> As molecular conformations are closely related to their physical properties and chemical reactivity, it is essential to understand the physical origin of the anomeric effect. Yet, no consensus has been reached so far, although extensive experimental and computational studies have been conducted in the past 50 years.<sup>6,7,14,18–43</sup> The currently popular hyperconjugation explanation initially came from the analysis of the X-ray crystallographic data with the longer substituent axial bonds

relative to  $C$ -substituent equatorial bonds.<sup>10</sup> It states that the preference of  $\alpha$  anomers is a manifestation of the charge delocalization from the lone pairs on  $X$  to the vacant antibonding orbital  $\sigma_{CY}^*$  (Scheme 1a), which reaches a maximum when group  $Y$  is in axial orientation.<sup>10,44–46</sup> The hyperconjugation model is consistent with the structural changes associated with the anomeric effect, since the  $n \rightarrow \sigma^*$  electron delocalization interaction tends to strengthen the  $X-C$  bond but weaken the  $C-Y$  bond. An alternative and conventional explanation is the electrostatic (dipole) model, 60

**Scheme 1. Hyperconjugation (a) and Electrostatic (b) Explanations of the Anomeric Effect**



**Received:** October 15, 2013

**Table 1.** Relative Energies ( $\Delta E_{\alpha \rightarrow \beta}$ ) and Delocalization Energies ( $DE^0$ , kcal/mol), Electron Population Changes on C1, X2, and Y, and Dipole Moments ( $\mu^0$ , Debye) for  $C_5XH_3Y^a$ 

Y	anomer	$\Delta E_{\alpha \rightarrow \beta}^b$			DE <sup>0</sup>	$\Delta P^{0c}$			$\mu$	
		MP2	HF	BLW		C1	X	Y	BLW	HF
(X = O)										
F	$\alpha$	0.00	0.00	0.00	35.01	0.033	−0.039	−0.010	2.729	2.509
	$\beta$	3.41	2.79	3.48	35.70	0.024	−0.029	−0.018	4.380	3.918
OH	$\alpha$	0.00	0.00	0.00	35.69	0.030	−0.028	−0.019	0.596	0.477
	$\beta$	1.32	0.77	2.22	37.14	0.025	−0.024	−0.026	3.003	2.481
Cl	$\alpha$	0.00	0.00	0.00	35.37	0.029	−0.038	−0.001	2.959	2.794
	$\beta$	2.70	2.46	1.80	34.71	0.020	−0.022	−0.016	4.341	3.871
NH <sub>2</sub>	$\alpha$	0.00	0.00	0.00	35.22	0.031	−0.018	−0.026	2.052	1.834
	$\beta$	−2.73	−3.08	−2.50	35.80	0.026	−0.017	−0.026	1.922	1.468
CH <sub>3</sub>	$\alpha$	0.00	0.00	0.00	29.77	0.015	−0.018	−0.007	1.955	1.771
	$\beta$	−3.30	−3.47	−2.30	30.94	0.014	−0.017	−0.011	2.010	1.715
(X = S)										
F	$\alpha$	0.00	0.00	0.00	28.95	0.027	−0.035	−0.007	2.769	2.509
	$\beta$	3.08	2.37	1.62	28.20	0.015	−0.019	−0.014	4.317	3.912
OH	$\alpha$	0.00	0.00	0.00	30.98	0.023	−0.025	−0.016	0.698	0.584
	$\beta$	2.72	1.99	1.95	30.94	0.017	−0.016	−0.021	3.013	2.562
Cl	$\alpha$	0.00	0.00	0.00	27.95	0.029	−0.038	−0.005	2.835	2.607
	$\beta$	1.40	1.02	0.28	27.21	0.021	−0.022	−0.016	4.240	3.813
CH <sub>3</sub>	$\alpha$	0.00	0.00	0.00	24.98	0.019	−0.026	−0.004	2.188	2.025
	$\beta$	−1.80	−2.02	−1.66	25.34	0.018	−0.025	−0.007	2.241	2.021

<sup>a</sup>All results were computed with the MP2/6-31+G(d) optimal geometries. <sup>b</sup>Relative energies are referenced to  $\alpha$  conformers at the same theoretical level. <sup>c</sup> $\Delta P^0 = P_{HF}^0 - P_{BLW}^0$ .

61 which was initially proposed by Edward to explain the  
62 destabilization of equatorial conformers of carbohydrates.<sup>1,47</sup>

63 The orientations and interactions of the local dipoles of the  
64 lone pairs on X and the C–Y polar bond favor  $\alpha$  anomers  
65 (Scheme 1b).

66 Obviously, both the hyperconjugation and electrostatic  
67 explanations have their justifications with certain experimental  
68 proofs. In particular, the  $n \rightarrow \sigma^*$  negative hyperconjugation  
69 explanation is in accord with geometric variations, though the  
70 electrostatic model can interpret this kind of geometrical  
71 changes to some extent as well.<sup>48</sup> The electrostatic model is  
72 mostly endorsed by the observation that the magnitude of the  
73 anomeric effect decreases when the solvent dielectric constant  
74 increases.<sup>49–52</sup> Though the hyperconjugation model enjoys its  
75 popularity, there have been recent evidence challenging this  
76 model.<sup>36,37,39,48,53–58</sup> A more balanced view, however, is that  
77 both steric and electronic interactions make contributions to  
78 the conformational preference.<sup>22,40</sup>

79 In the recent years, we have been developing the block-  
80 localized wave function (BLW) method<sup>59,60</sup> which is the most  
81 simplified and efficient variant of the valence bond (VB)  
82 theory,<sup>61–63</sup> in attempt to quantify the electron delocalization  
83 (conjugation and hyperconjugation) effect and differentiate it  
84 from the steric effect (broadly defined here as we interpret it as  
85 a sum of Pauli exchange repulsion and electrostatic  
86 interactions) at the quantum mechanical level. Compared  
87 with existing post-SCF analysis schemes,<sup>64–66</sup> the BLW method  
88 uniquely defines a hypothetical electron-localized Lewis state  
89 whose wave function is self-consistently optimized and taken as  
90 a reference for the measure of the electron delocalization. This  
91 is achieved by limiting the expansion of one-electron molecular  
92 orbitals.<sup>67–73</sup> Our applications to the exemplary systems for the  
93 anomeric effect, namely, dimethoxymethane and substituted  
94 tetrahydropyrans, provided strong computational evidence that  
95 disapprove the hyperconjugation explanation for the anomeric

effect.<sup>36,39</sup> Most recently, we investigated the generalized  
96 anomeric effect in a series of systems, and found that the  
97 hyperconjugation effect contributes to the conformational  
98 preference in certain systems, while in others it plays a negative  
99 role in the conformational preference, and the steric effect thus  
100 is solely responsible for the generalized anomeric effect.<sup>40</sup>  
101 Considering that the hyperconjugation effect is not exper-  
102 imentally measurable, and only the solvent effect can be  
103 quantified in the wet lab, we feel that applications of the BLW  
104 method in the solvent environment may provide further  
105 insights into the nature of the anomeric effect.  
106

Experimentally, distributions of different anomers can be  
107 measured by optical rotation and NMR experiments.<sup>74–76</sup> Praly  
108 and Lemieux probed the influence of solvent polarity and  
109 hydrogen bond formation on the conformational preference for  
110 2-substituted tetrahydropyrans using NMR and showed that  $\beta$   
111 anomers are significantly favored by water, primarily due to the  
112 hydrogen bonding interactions between the anomeric groups  
113 and solvent water molecules.<sup>50</sup> For the instance of 2-methoxy  
114 tetrahydropyran, 83% of the molecules adopt the axial  
115 conformation in the nonpolar solvent CCl<sub>4</sub> but only 52% lie  
116 axial in water.<sup>49</sup> However, there are also anomeric systems such  
117 as 2-carbomethoxy-1,3-dithiane in which increasing the polarity  
118 of the solvent favors axial conformation.<sup>77</sup> With the enormous  
119 experimental measurements of the solvent effect on the  
120 equilibrium between  $\alpha$  and  $\beta$  anomers, computational studies  
121 have also been conducted in order to elucidate the forces  
122 governing the anomeric effect and reconcile the differential  
123 behaviors of different anomeric systems in solution.<sup>51,52</sup>  
124 Because of the complexity of solvent structures, most works  
125 are based on implicit solvent models, notably the polarized  
126 continuum model (PCM).<sup>78–80</sup> For instance, Carballeira and  
127 Pérez-Juste probed the conformational preferences of methyl-  
128 enediamine and several methylated derivatives in the gas phase  
129 and aqueous solution.<sup>81,82</sup> They claimed that the charge 130

delocalization is the main cause for the anomeric effect based on the NBO analysis, and PCM computations showed that the anomeric effect is not reduced but enlarged in water, though the electrostatic interaction is largely responsible for the energetic changes, and depends strongly on local solute–solvent interactions. Vila and co-workers developed an interpretative model based on the quantum theory of atoms in molecules (QTAIM)<sup>64</sup> for the anomeric effect<sup>57</sup> and analyzed a number of anomeric systems in three solvents.<sup>83</sup> They found that atomic electron population reorganization in different conformers of each molecule decreases when the polarity of the solvent increases, and both the electron density variation and conformational preference can be interpreted by the repulsion between the hydrogen atoms and lone pair orbitals.

In this work, we combined the BLW method with the PCM approach and decomposed the conformational energy differences at the MP2 level into three components, namely, the electron delocalization energy ( $\Delta E^S$ ), steric effect ( $\Delta E_s$ ), and electron correlation ( $\Delta E_c$ ). While this decomposition scheme seems similar to our previous one in gas phase,<sup>36,39,40</sup> here either of the delocalization energy or steric energy is composed of two contributions, namely, the intrinsic energy term and a secondary energy term induced by the solute–solvent interactions. This BLW-PCM scheme was applied to substituted tetrahydropyrans  $C_5OH_9Y$  ( $Y = F, Cl, OH, NH_2$ , and  $CH_3$ ) and tetrahydrothiopyrans  $C_5SH_9Y$  ( $Y = F, Cl, OH$ , and  $CH_3$ ) in solvents including chloroform (clform in short in the following), acetone, and water in order to gain insights into the physical origin of the anomeric effect. Computations in gas phase were performed for comparison. The variation of the total dipole moment caused by the solvent effect, as well as the differences in solute–solvent interaction energy and dipole moment between  $\alpha$  and  $\beta$  conformers were also investigated, for the purpose of identifying the cause for the change of the anomeric effect in polar solvents.

## RESULTS AND DISCUSSION

**Anomeric Effect in Gas Phase.** We first performed computations of the systems in gas phase. Note that substituted tetrahydropyrans  $C_5OH_9Y$  ( $Y = F, Cl, OH, NH_2$ , and  $CH_3$ ) previously were analyzed by one of us.<sup>36</sup> For the sake of consistency of this work, we revisited these cases, and the only difference from the previous work is the adoption of the frozen core approximation here, which leads to tiny changes of both the relative energy and delocalization energy less than 0.05 kcal/mol. Table 1 listed the relative conformational energies, delocalization energies, dipole moments, and electron population changes from electron-localized (BLW) to delocalized (HF) states. As found previously, the delocalization energies in  $\alpha$  and  $\beta$  conformers are comparable for all substituted tetrahydropyrans, while the  $\beta$  conformers are even more stabilized by the intramolecular electron delocalization particularly when  $Y = F$  and  $OH$ . Thus, the results for 2-fluorotetrahydropyran and 2-tetrahydropyranol are inconsistent with the hyperconjugation explanation. But we reiterate that both the  $n \rightarrow \sigma^*$  negative hyperconjugative interaction and the geminal interactions are included in the delocalization energy, which generally cannot be separated effectively (however, Khaliullin et al.<sup>73</sup> have proposed a solution using a perturbative approximation where the delocalization energy is composed of a single noniterative Roothaan step (RS) and a higher order

relaxation (induction), and the RS term is a sum of occupied-virtual pairwise energies).

A more sensitive measure may be the electron population changes on the anomeric center C1 and O2, as well as the substituent Y. Table 1 indicated that in all anomeric or nonanomeric molecules, with the electron delocalization, there is a reduction of the electron population on the endocyclic oxygen atom O2, which is in accord with the hyperconjugation model and confirms the  $n(O2) \rightarrow \sigma^*(CY)$  electron flow. But we note that geminal interactions also contribute to the population changes. Interestingly, the populations on Y decrease as well with the electron delocalization, indicating the hyperconjugation from Y to the C1–O2 and C1–C5 antibonds. Such kind of hyperconjugation broadly exists even in ethane.<sup>84</sup> The population on the anomeric carbon, however, increases in all cases. Significantly, O2 loses more electrons in the  $\alpha$  anomer than in the  $\beta$  anomer for each molecule, confirming a stronger  $n(O2) \rightarrow \sigma^*(CY)$  hyperconjugative interaction in the former. In contrast, there is more significant electron loss from Y in the  $\beta$  anomer than in the  $\alpha$  anomer, suggesting a competing  $n(Y) \rightarrow \sigma^*(CO)/\sigma^*(CC)$  hyperconjugation, also called exoanomeric effect. While the  $n(O2) \rightarrow \sigma^*(CY)$  interaction is usually more pronounced than  $n(Y) \rightarrow \sigma^*(CO)/\sigma^*(CC)$  interaction, one exception is 2-amino-tetrahydropyran, which is well recognized for the preference of the  $\beta$  anomer over the  $\alpha$  anomer, a phenomenon sometimes called reverse anomeric effect (which usually refers to cationic substituents).<sup>4,19,22,85–87</sup> Steric repulsions have been cited as the cause.<sup>23,88</sup> Here we found that among all substituted tetrahydropyrans, 2-aminotetrahydropyran is the only one with more electron loss on Y than on O2, suggesting a more significant exoanomeric effect than the regular endoanomeric effect. This can be explained by the slightly low electronegativity of nitrogen compared with fluorine and oxygen, which makes the amine group a good electron donor and the C–N antibond orbital a poor electron acceptor. The change of electron density from the electron-localized state to the electron-delocalized state better be visualized with electron density difference (EDD) maps. Figure 1 shows the electron

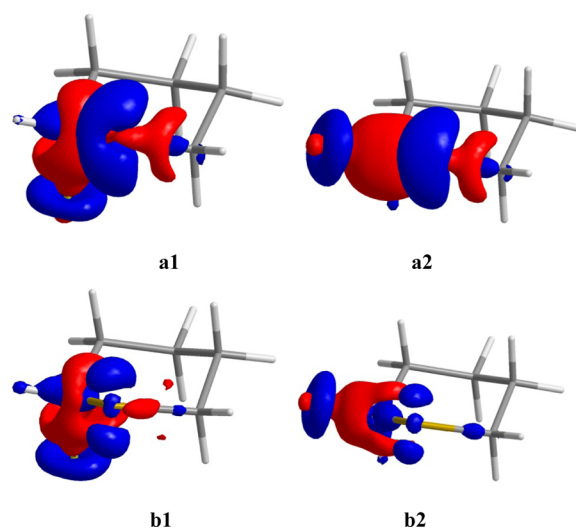


**Figure 1.** Intramolecular electron delocalization shown by the electron density difference (EDD) maps for the  $\alpha$  and  $\beta$  conformers of  $C_5OH_9F$  (a) and  $C_5SH_9F$  (b) with isodensity value 0.002 au. The red/blue color means an increase/reduction of electron density.



delocalization effect in the  $\alpha$ - and  $\beta$ -conformers of  $C_5OH_9F$  and  $C_5SH_9F$ , where the red color indicates a gain and the blue denotes a loss of electron density. EDD maps clearly show that the electron delocalization interactions mainly occur on the C1, O2, and Y atoms or group.

Overall, the magnitude of the anomeric effect decreases in the order of  $F > Cl > OH > NH_2 > CH_3$ , which is approximately in the same order as the  $\Delta P^0$  values of  $\alpha$  conformers. Our calculations also showed that population change is reduced when the endocyclic oxygen is substituted by a sulfur atom. For the example of  $C_5OH_9F$ , population changes on O2 are 0.004 and 0.010 e more than those on S2 of  $C_5SH_9F$  for the  $\alpha$  and  $\beta$  conformers. This finding can be confirmed by EDD maps as demonstrated in Figure 1. With the same isodensity value, it is obvious that there are more electrons delocalized in  $C_5OH_9F$  than in  $C_5SH_9F$ . Analyses based on the electron density distribution so far suggest that the hyperconjugation effect is the primary culprit for the anomeric effect. However, it must be noted that conformational preferences are unchanged after the complete removal of all electron delocalization interactions in BLW computations. In other words, the EDD maps show the trends but cannot measure the weight of the hyperconjugative interactions in the conformational preference for anomeric systems studied in this work.

Among the four substituted tetrahydrothiopyrans studied in this work,  $\alpha$  anomers are favored for  $Y = F, OH$ , and  $Cl$ , and thus exemplify the anomeric effect. In contrast, for  $C_5SH_9CH_3$ , the  $\beta$  anomer is about 2 kcal/mol more stable than the  $\alpha$  anomer. Thus,  $C_5SH_9CH_3$  does not exhibit the anomeric effect and can be taken as a reference. In both substituted tetrahydropyrans and tetrahydrothiopyrans, the energy gap between  $\alpha$  and  $\beta$  anomers are enlarged by the MP2 method, indicating the importance of the electron correlation for the conformational behavior, which favor more crowded conformers in terms of dispersion effect. For the instance of  $C_5SH_9F$ , the  $\alpha$ - $\beta$  conformational energy difference with the HF method is 2.37 kcal/mol, while MP2 method increases it to 3.08 kcal/mol. Compared with  $C_5OH_9Y$  with the exception of  $Y = OH$ ,  $C_5SH_9Y$  has relatively low  $\alpha$ - $\beta$  conformational energy gap.

As the intramolecular electron delocalization reduces the electron populations on O2 and Y but increases the populations on the anomeric carbon C1 (Table 1), it is rational to conclude that the electron delocalization reduces the local dipoles as illustrated in Scheme 1b. Table 1 listed the overall molecular dipole moments in the electron-localized (BLW) and electron-delocalized (HF) states. Two significant characteristics of the dipole moments in Table 1 can be observed. One is the much higher dipole moment of a  $\beta$  anomer than its corresponding  $\alpha$  anomer except 2-aminotetrahydropyran with the reverse anomeric effect. Besides, in both  $C_5OH_9CH_3$  and  $C_5SH_9CH_3$ , the dipole moments of  $\alpha$  and  $\beta$  anomers are similar. The second feature is the good correlation between the dipole moments in electron-localized and electron-delocalized states, as shown in Figure 2.

**Anomeric Effect in Solution.** The relative energy  $\Delta E_{\alpha\rightarrow\beta}$  of  $\alpha$  and  $\beta$  anomers in chloroform (dielectric constant  $\epsilon = 4.8$ ), acetone ( $\epsilon = 20.7$ ), and water ( $\epsilon = 80.4$ ) were computed at MP2, HF, and BLW levels for molecules  $C_5OH_9Y$  ( $Y = F, Cl, OH, NH_2$ , and  $CH_3$ ) and  $C_5SH_9Y$  ( $Y = F, Cl, OH$ , and  $CH_3$ ). The solvent effect is modeled via the PCM approach, and Table 2 summarizes the magnitudes of the conformational preference. In agreement with previous experimental and computational

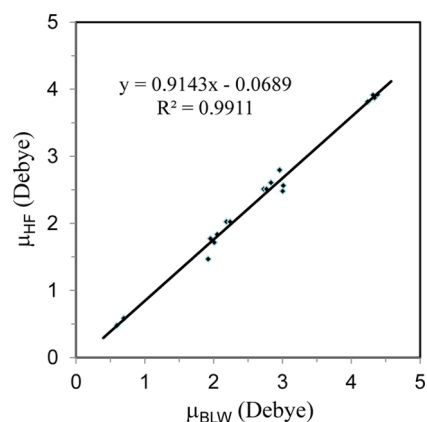


**Figure 2.** Correlation between the total dipole moment of the electron-localized and electron-delocalized states of  $\alpha$  and  $\beta$  anomers of  $C_5OH_9Y$  and  $C_5SH_9Y$ .

**Table 2.** Energy Difference ( $\Delta E_{\alpha\rightarrow\beta}$ , kcal/mol) between  $\alpha$  and  $\beta$  Anomers of  $C_5XH_9Y$  at the MP2, HF, and BLW Levels of Theory in Gas Phase and Solution

Y	level	$\Delta E_{\alpha \rightarrow \beta}$			
		vac	clform	acetone	water
(X = O)					
F	MP2	3.41	2.54	2.29	2.23
	HF	2.79	1.75	1.47	1.40
	BLW	3.48	1.94	1.55	1.46
OH	MP2	1.32	0.53	0.31	0.26
	HF	0.77	-0.09	-0.32	-0.38
	BLW	2.22	0.88	0.55	0.47
Cl	MP2	2.70	2.02	1.84	1.79
	HF	2.46	1.69	1.48	1.43
	BLW	1.80	0.75	0.47	0.47
NH <sub>2</sub>	MP2	-2.73	-2.67	-2.64	-2.63
	HF	-3.08	-3.02	-3.00	-2.99
	BLW	-2.50	-2.76	-2.63	-2.57
CH <sub>3</sub>	MP2	-3.30	-3.24	-3.23	-3.23
	HF	-3.47	-3.41	-3.40	-3.40
	BLW	-2.30	-2.34	-2.36	-2.36
(X = S)					
F	MP2	3.08	2.72	2.60	2.57
	HF	2.37	1.98	1.85	1.82
	BLW	1.62	1.07	0.91	0.87
OH	MP2	2.72	1.56	1.26	1.19
	HF	1.99	0.82	0.52	0.45
	BLW	1.95	0.54	0.19	0.10
Cl	MP2	1.40	1.02	0.90	0.87
	HF	1.02	0.62	0.49	0.46
	BLW	0.28	-0.31	-0.49	-0.49
CH <sub>3</sub>	MP2	-1.80	-1.78	-1.77	-1.77
	HF	-2.02	-2.00	-2.00	-2.00
	BLW	-1.66	-1.60	-1.60	-1.60

results, Table 2 shows that for the molecules exhibiting the anomeric effect ( $Y = F, OH, Cl$ ), the conformational preference is diminished in solutions, and the magnitude of reduction increases as the solvent polarity increases. Of course, these data coincide with the electrostatic explanation of the anomeric effect. For example, the  $\alpha$  anomer of  $C_5OH_9F$  is 3.41 kcal/mol more stable than the  $\beta$  anomer in gas phase, but the energy gap is reduced to 2.23 kcal/mol in water. For those non- or reverse

**Table 3. Intramolecular Delocalization Energies (kcal/mol) in Gas Phase and Solution and Electron Population Changes from Gas Phase to Aqueous Solution for  $\alpha$  and  $\beta$  Conformers of  $C_5XH_9Y$** 

		DE <sup>SO</sup>				$\Delta P^{Sa}$		
Y	anomer	vac	clform	acetone	water	C1	X	Y
(X = O)								
F	$\alpha$	35.01	35.01	35.01	35.02	0.003	0.018	0.017
	$\beta$	35.70	35.74	35.77	35.78	0.006	0.027	0.021
OH	$\alpha$	35.69	35.67	35.67	35.37	0.001	0.017	0.005
	$\beta$	37.14	37.17	37.20	36.95	0.005	0.021	0.013
Cl	$\alpha$	35.37	35.32	35.31	35.32	0.027	0.007	−0.079
	$\beta$	34.71	34.76	34.78	34.85	−0.002	0.025	0.028
NH <sub>2</sub>	$\alpha$	35.22	35.36	35.40	35.45	0.001	0.022	0.001
	$\beta$	35.80	35.75	35.92	36.02	0.003	0.020	0.006
CH <sub>3</sub>	$\alpha$	29.77	29.77	29.77	29.77	0.000	0.025	−0.005
	$\beta$	30.94	30.94	30.95	30.95	0.003	0.025	0.001
(X = S)								
F	$\alpha$	28.95	28.94	28.94	28.94	0.001	0.028	0.018
	$\beta$	28.20	28.19	28.19	28.19	0.002	0.042	0.021
OH	$\alpha$	30.98	30.96	30.95	30.95	−0.002	0.027	0.006
	$\beta$	30.94	30.96	30.96	30.97	0.001	0.036	0.011
Cl	$\alpha$	27.95	28.06	28.19	28.08	−0.004	0.027	0.023
	$\beta$	27.21	27.24	27.43	27.32	−0.005	0.041	0.026
CH <sub>3</sub>	$\alpha$	24.98	24.87	24.84	24.84	−0.005	0.045	−0.005
	$\beta$	25.34	25.31	25.30	25.29	−0.004	0.043	−0.001

$$^a \Delta P^S = P_{HF}^S - P_{HF}^0.$$

anomeric systems ( $C_5OH_9NH_2$ ,  $C_5OH_9CH_3$ , and  $C_5SH_9CH_3$ ) where  $\beta$  conformers are preferred, the  $\alpha$ – $\beta$  energy gap has little dependence on the solvent effect. Similar to the trend in gas phase, the relative stabilization of  $\alpha$  anomers is reinforced by the electron correlation. Thus, for anomeric molecules, the energy gaps are enlarged, but for non- and reverse anomeric systems, the energy gaps are reduced at the MP2 level compared with the HF level. In general, the solvent effect is not strong enough to change the ordering of the energy gap for substituted tetrahydropyrans and tetrahydrothiopyrans. In other words, in both gas phase and solutions, the magnitude of the conformational preference for  $C_5OH_9Y$  decreases in the order of  $F > Cl > OH > NH_2 > CH_3$ , and for  $C_5SH_9Y$  the order is  $F > OH > Cl > CH_3$ .

At the outset, it seems that the reduction of the conformational preference in solution can also be explained by the hyperconjugation model. Because of the hydrogen bonding interaction and/or polarization with solvent molecules, the endocyclic O2 (S2) has a lowered propensity of giving or accepting electron density, resulting in the reduction of both the endo- and exoanomeric effect. However, there are two outstanding findings from the electron-localized state (BLW) calculations in solvent that are inconsistent with the hyperconjugation explanation. First, with the removal of intramolecular electron delocalization, the conformational preference remains unchanged for all systems, as both the BLW and HF (or MP2) computations lead to the same trends. One partial exception is  $C_5OH_9OH$ , for which the  $\beta$  anomer is favored in chloroform, acetone, and water at the HF level, but both the BLW and MP2 computations favor the  $\alpha$  anomer in all environments. In this case, the electron delocalization plays a negative role for the anomeric effect in  $C_5OH_9OH$ . Second, the dependence of the energy gap between  $\alpha$  and  $\beta$  anomers on the solvent polarity can be seen even when all electron delocalization is quenched. In other words, similar to the MP2 and HF results, BLW computations also show that the

energy gap decreases with the increasing polarity for the anomeric systems  $C_5XH_9Y$  ( $X = O, S$ ;  $Y = F, OH, Cl$ ). These two observations suggest that neither the conformational preference nor its variation in different environment is uniquely determined by the hyperconjugation effect, which is in accord with our findings in gas phase.

Although the hyperconjugative interaction does not play a determining role in the anomeric effect, it does make non-negligible contributions in an either positive (enhancing the anomeric effect) or negative (diminishing the anomeric effect) way. It is thus worthwhile to look into the electron delocalization in more details. Equation 8 shows that the delocalization energy in solution can be decomposed to two parts: one is the intrinsic intramolecular delocalization energy (DE<sup>SO</sup>), and the other is the secondary energy change (SE<sup>V</sup>) due to the solute–solvent interactions. Table 3 compiles the absolute values of the intrinsic delocalization energies for both  $\alpha$  and  $\beta$  anomers in solution computed with the BLW method. The hyperconjugation model for the anomeric effect would expect reduced hyperconjugative interactions and subsequently reduced intrinsic delocalization energy in solution compared with in gas phase. However, Table 3 demonstrated that for all molecules in all media, the intrinsic delocalization energy has little changes. For the example of the  $\alpha$  anomer of  $C_5OH_9F$ , the total energy changes by 0.67 kcal/mol from gas phase to water at the HF level. But the variation of the delocalization energy is merely 0.01 kcal/mol. We note, nevertheless, that short-range hydrogen bonds between solute and solvent are not explicitly considered in the PCM model (examples with explicit water molecules will be discussed in the following subsection). The population change  $\Delta P^S$  in Table 3 measures the electron density changes due to the solvent effect, and we indeed observe the increase of the electron population on the endocyclic O2 or S2, which does not translate to the increase of intrinsic delocalization energy. A visualization of the overall electron density change due to the solvent effect is sampled in

Figure 3, which corresponds to the density difference between a molecule in water and in gas phase.

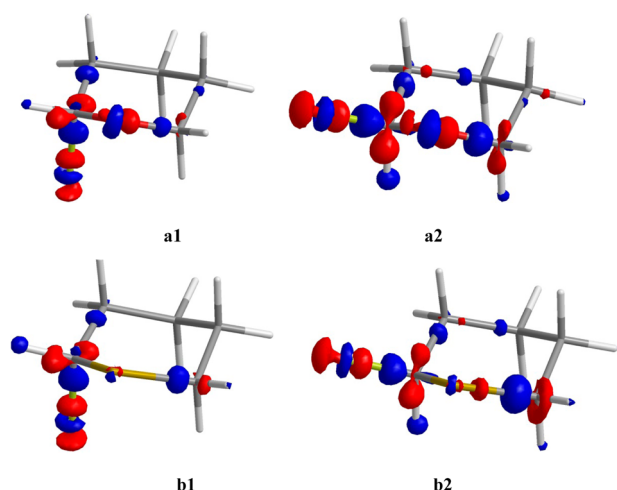


**Figure 3.** Electron density polarization in water shown by the electron density difference (EDD) maps for the  $\alpha$  and  $\beta$  conformers of  $C_5OH_9F$  (a) and  $C_5SH_9F$  (b) with isodensity value 0.002 au. The red/blue color means an increase/reduction of electron density.

As the total delocalization energy in solution is contributed by two components (eq 8), the energy difference between  $\alpha$  and  $\beta$  anomers in solution is similarly composed of two contributions. Table 4 listed the impacts of both the intrinsic electron delocalization and the solute–solvent interaction induced delocalization on the conformational preference of the studied systems in this work. We first look at the term of total delocalization interaction  $\Delta DE^S$ . In cases of  $C_5SH_9Y$  ( $Y = F, OH, \text{ and } Cl$ ), the total delocalization energies in  $\alpha$  anomers are higher than in their corresponding  $\beta$  anomers in all solvents, suggesting that the total hyperconjugative interactions positively contribute to the anomeric effect. However, for all  $C_5OH_9Y$  except  $Y = Cl$ , electron delocalization stabilizes  $\beta$  anomers more than  $\alpha$  anomers in solution, and thus negatively contributes to the anomeric effect. This is consistent with the previous study in gas phase<sup>36</sup> and suggests the steric (electrostatic) explanation for the conformational preference. It is also interesting to see that  $\Delta SE^V$  is negative in all cases of this work, indicating that the solute–solvent interaction reduces

the electron delocalization in  $\beta$  anomers more than  $\alpha$  anomers. Note that delocalization is a stabilizing force and the reduction of delocalization thus destabilizes a system.

The overall redistribution of the electron density of a molecule induced by solvation (Figure 3) can be signified by the change of its dipole moment. We compared the molecular dipole moments calculated in gas phase ( $\mu^0$ ) and solution ( $\mu^S$ ) and correlated them in the form of  $\mu^S = k\mu^0 + b$ , as shown in Figure 4. We note that  $k$  in all solvents is greater than 1, which

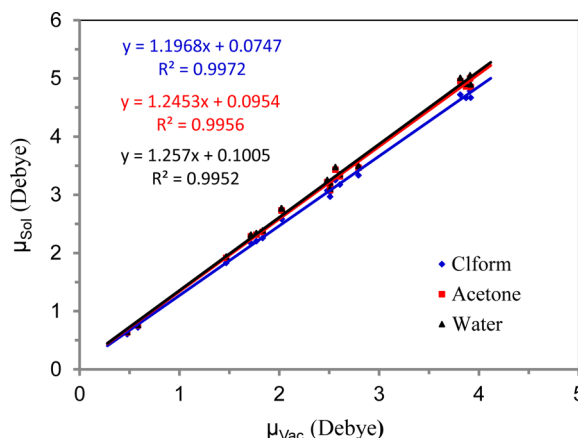


**Figure 4.** Correlation between the total dipole moments in gas phase and in solution for  $\alpha$  and  $\beta$  anomers of  $C_5XH_9Y$ .

means all anomers undergo polarization in solutions. Computations have shown that a  $\beta$  anomer has higher dipole moment and subsequently is polarized more than its corresponding  $\alpha$  anomer. For the example of the  $\beta$  anomer of  $C_5OH_9F$ , its total dipole moment is increased by 0.979 D in water, which is 0.383 D higher than the  $\alpha$  anomer. Interestingly, the value of  $k$  increases with the solvent polarity increasing. Hence,  $k$  reflects the ability of solvent molecules to polarize the solute, and as we expect, the solvent with higher polarity tends to polarize the solute molecule more. In brief, molecular dipole moment is lowered by the intramolecular electron delocalization but enhanced by the solvent effect.

According to Figure 4, a  $\beta$  anomer would enhance its dipole moment more than the  $\alpha$  anomer in solution as the former has higher intrinsic dipole moment. Thus, the  $\beta$  anomer would be stabilized more than the  $\alpha$  anomer, and consequently, the

**Table 4.** Delocalization Energy Difference ( $\Delta DE^S$ )<sup>a</sup> between  $\alpha$  and  $\beta$  Anomers of  $C_5XH_9Y$  in Solution with Decomposed Contributions from Intrinsic Delocalization and Solute–Solvent Interaction Energy Changes (kcal/mol)

Y	clform			acetone			water		
	$\Delta DE^{S0}$	$\Delta SE^V$	$\Delta DE^S$	$\Delta DE^{S0}$	$\Delta SE^V$	$\Delta DE^S$	$\Delta DE^{S0}$	$\Delta SE^V$	$\Delta DE^S$
(X = O)									
F	0.73	−0.54	0.19	0.76	−0.68	0.08	0.77	−0.71	0.06
OH	1.50	−0.52	0.98	1.53	−0.66	0.87	1.58	−0.73	0.85
Cl	−0.56	−0.38	−0.94	−0.54	−0.48	−1.01	−0.46	−0.50	−0.97
NH <sub>2</sub>	0.39	−0.13	0.26	0.51	−0.14	0.37	0.57	−0.15	0.41
CH <sub>3</sub>	1.17	−0.10	1.06	1.18	−0.14	1.04	1.18	−0.14	1.04
(X = S)									
F	−0.75	−0.16	−0.91	−0.75	−0.19	−0.94	−0.75	−0.20	−0.94
OH	0.00	−0.28	−0.28	0.01	−0.34	−0.33	0.02	−0.36	−0.34
Cl	−0.82	−0.11	−0.93	−0.76	−0.22	−0.98	−0.76	−0.19	−0.95
CH <sub>3</sub>	0.44	−0.04	0.40	0.46	−0.06	0.40	0.45	−0.06	0.39

<sup>a</sup> $\Delta DE = DE(\beta) - DE(\alpha)$ .

**Table 5. Steric Energy Difference ( $\Delta E_s$ )<sup>a</sup> between  $\alpha$  and  $\beta$  Anomers of  $C_5XH_9Y$  in Solution with Decomposed Contributions from Intrinsic Steric Effect and Solute–Solvent Interaction Energy Changes (kcal/mol)**

Y	clform			acetone			water		
	$\Delta E_s^{S0}$	$\Delta E_s^V$	$\Delta E_s$	$\Delta E_s^{S0}$	$\Delta E_s^V$	$\Delta E_s$	$\Delta E_s^{S0}$	$\Delta E_s^V$	$\Delta E_s$
(X = O)									
F	3.82	−1.88	1.94	4.02	−2.47	1.55	4.07	−2.61	1.46
OH	2.50	−1.62	0.88	2.67	−2.12	0.55	2.76	−2.29	0.47
Cl	2.12	−1.37	0.75	2.27	−1.80	0.47	2.37	−1.90	0.47
NH <sub>2</sub>	−2.74	−0.02	−2.76	−2.65	0.02	−2.63	−2.60	0.03	−2.57
CH <sub>3</sub>	−2.28	−0.07	−2.34	−2.25	−0.11	−2.36	−2.25	−0.11	−2.36
(X = S)									
F	1.83	−0.76	1.07	1.97	−1.05	0.91	2.01	−1.13	0.87
OH	2.27	−1.73	0.54	2.44	−2.26	0.19	2.50	−2.40	0.10
Cl	0.32	−0.62	−0.31	0.36	−0.84	−0.49	0.41	−0.90	−0.49
CH <sub>3</sub>	−1.57	−0.02	−1.60	−1.56	−0.04	−1.60	−1.56	−0.04	−1.60

$$^a\Delta E_s = E_{BLW}^S(\beta) - E_{BLW}^S(\alpha).$$

**Table 6. Decomposition of the  $\alpha$ – $\beta$  Energy Gap for  $C_5XH_9Y$  (kcal/mol)**

Y	clform			acetone			water		
	$\Delta E_{HF}^{S0}$	$\Delta E_{HF}^V$	$\Delta E_C$	$\Delta E_{HF}^{S0}$	$\Delta E_{HF}^V$	$\Delta E_C$	$\Delta E_{HF}^{S0}$	$\Delta E_{HF}^V$	$\Delta E_C$
(X = O)									
F	3.09	−1.34	0.79	3.26	−1.79	0.82	3.31	−1.91	0.83
OH	1.00	−1.10	0.62	1.14	−1.46	0.63	1.18	−1.56	0.64
Cl	2.67	−0.99	0.33	2.80	−1.32	0.35	2.84	−1.40	0.36
NH <sub>2</sub>	−3.13	0.11	0.35	−3.16	0.16	0.35	−3.17	0.18	0.35
CH <sub>3</sub>	−3.45	0.04	0.17	−3.43	0.03	0.17	−3.43	0.03	0.17
(X = S)									
F	2.58	−0.60	0.75	2.72	−0.87	0.75	2.76	−0.94	0.76
OH	2.27	−1.45	0.74	2.43	−1.92	0.74	2.48	−2.03	0.74
Cl	1.23	−0.61	0.40	1.37	−0.87	0.40	1.40	−0.94	0.41
CH <sub>3</sub>	−2.01	0.01	0.22	−2.01	0.02	0.23	−2.01	0.01	0.23

anomeric effect would be reduced, as both experiments and computations have shown. To gain more insights into the change of the anomeric effect in solution, we decompose the steric effect in solution ( $\Delta E_s$ ) to the intrinsic steric effect ( $\Delta E_s^{S0}$ ) and the secondary effect due to the solute–solvent interactions ( $\Delta E_s^V$ ), as expressed in eq 11. Table 5 compiles results. In all cases, the intrinsic steric effect, which is a combination of intramolecular electrostatic and Pauli repulsion, increases slightly along with the solvent polarity. But this very modest increasing is overwhelmed by the solute–solvent interaction, which increases much more rapidly with the solvent polarity. As a consequence, the steric interaction in solution reduces. This reduction is ultimately responsible for the reduced anomeric effect.

Alternatively, we can partition the MP2 energy difference in terms of intrinsic HF energy difference ( $\Delta E_{HF}^{S0}$ ), solvation energy difference at the HF level ( $\Delta E_{HF}^V$ ), and the correlation energy ( $\Delta E_C$ ) as shown in eq 10. Table 6 listed the data. Of significance, we find that  $\Delta E_{HF}^{S0}$  and  $\Delta E_{HF}^V$  have contrasting roles in all systems. In other words, in anomeric systems (with positive values of  $\Delta E_{HF}^{S0}$ ), the  $\Delta E_{HF}^V$  terms are negative and thus reduce the magnitude of the anomeric effect. On the other hand, for non- or reverse anomeric systems, the  $\Delta E_{HF}^{S0}$  terms are negative and the  $\Delta E_{HF}^V$  terms are positive. Either way, the solute–solvent interactions tend to reduce the  $\alpha$ – $\beta$  energy gaps. Therefore, the reduction of anomeric effect in polar solvents is solely caused by the solute–solvent interaction energy.

**$C_5OH_9F$  with Explicit Water Molecule(s).** Continuum solvation models are known for being unable to properly describe the hydrogen bonding between solute and solvent molecules. For the systems studied in this work, both the endocyclic oxygen O2 and the electronegative substituent Y can form strong hydrogen bonds with adjacent water molecules. To evaluate the impact of the use of the PCM method in this work on our analyses and final conclusion, we take  $C_5OH_9F$  as an example to probe the  $\alpha$ – $\beta$  energy gap by explicitly including one or two water molecules in computations. As both O2 and F can serve as the hydrogen bond acceptors, we investigated three models as shown in Figure 5. Model 1 (M1) and 2 (M2) concern the hydrogen bonding interaction of O2 or F with one water molecule, while M3 includes both kinds of hydrogen bonds. Table 7 compiles the main computational results.

Table 7 shows that the hydrogen bonding of a solvent molecule to the endocyclic O2 reduces the anomeric effect at both MP2 and HF levels, whereas hydrogen bonding to the substituent (F) enhances the anomeric effect. The former reduction is more significant than the latter enhancement. When both types of hydrogen bonds are considered in model M3, the anomeric effect reduces as we have found with the PCM method in the previous subsection. If there are more explicit water molecules included in the computations, we expect that the magnitude of reduction will increase. These results are consistent with the hyperconjugation effect, as the depletion of the electron density on O2 due to the hydrogen bond in model M1 will reduce the  $n \rightarrow \sigma^*$  hyperconjugative interaction, while the attraction of F by the positively charged



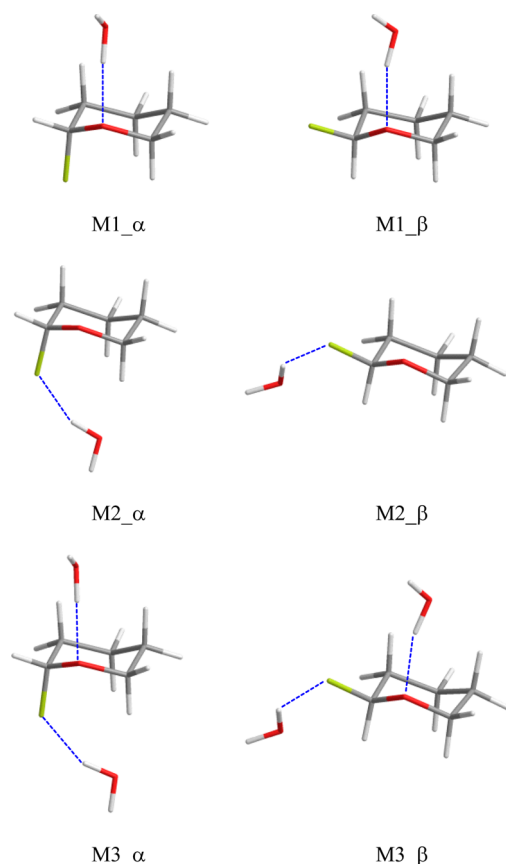


**Figure 5.** Optimal geometries of  $C_5OH_9F$  complexed with one or two water molecules at the MP2/6-31+G(d) level of theory.

electron transfer in the hydrogen bond is also quenched. In all electron-localized states, the preference of  $\alpha$  anomer still holds, suggesting that the hyperconjugation is not the origin of anomeric effect in water. The comparison between the  $\alpha$ - $\beta$  energy gaps with the HF and BLW methods shows that the electron delocalization enhances the anomeric effect, different from the PCM computations (Table 2), which show a reduction of anomeric effect in water for  $C_5OH_9F$ . A further analysis indicates that the intermolecular electron transfer in the formation of hydrogen bonds between  $C_5OH_9F$  and water molecule(s) is responsible for the discrepancy. We expect that the inclusion of more explicit water molecules in computations would generate results comparable with the PCM results presented in the previous subsection.

## CONCLUSION

The solution to the controversy over the nature of the anomeric effect lies in the proper estimates of the hyperconjugative and electrostatic interactions. Following the ab initio VB theory, we have developed the BLW method, which can derive the wave function for an electron-localized state where intramolecular electron delocalization is quenched. Although such kind of electron-localized state or resonance state is not a real physical state, it provides a useful theoretical reference state to differentiate the hyperconjugation and steric (including the electrostatic) effects, and is in line with conventional chemistry theory in terms of Lewis structure and resonance concept. Applying the BLW method to the anomeric effect, we have profoundly demonstrated that the hyperconjugation can play either positive or negative roles in the conformational preferences of various anomeric and generalized anomeric systems.<sup>36,39,40</sup> But even when the hyperconjugation effect plays a positive role, it contributes less than 50% to the  $\alpha$ - $\beta$  energy gap. Thus, we conclude that the steric effect, or more specifically the electrostatic interaction, dominates the anomeric effect.

Previous experiments have profoundly shown that in polar solvent the anomeric effect is diminished along with the solvent polarity. This phenomenon is further confirmed by numerous computational studies. It would be valuable to explore the electron-localized states in solution. As such, in this work we combined the BLW method with the PCM model and performed BLW-PCM analyses of a series of substituted tetrahydropyran and tetrahydrothiopyran in the solutions of chloroform, acetone, and water. Following the previous energy partition scheme in gas phase, we can decompose the  $\alpha$ - $\beta$  energy gap in solution to the contributions from intramolecular

hydrogen atom of water in model M2 enhances the hyperconjugation. However, the examination of hydrogen bonding interactions ( $\Delta E_b$  in Table 7) reveals that the changes of the  $\alpha$ - $\beta$  energy gap in all models dominantly result from the variation of hydrogen bonding energy. For instance, with the bonding of one water molecule to O2, the  $\alpha$ - $\beta$  energy gap at the MP2 level reduces from 3.41 to 2.41 kcal/mol by 1.00 kcal/mol, but the difference of the hydrogen bond strength in  $\alpha$  and  $\beta$  anomers contributes 0.83 kcal/mol. This finding supports our conclusion based on the PCM model that the solute-solvent interactions, rather than the intrinsic electron delocalization (hyperconjugation), cause the variation of anomeric effect.

In the BLW computations of models M1, M2, and M3, we treat each water molecule as one individual block; thus, the

**Table 7.** Energy Differences ( $\Delta E_{\alpha \rightarrow \beta}$ ) between  $\alpha$  and  $\beta$  Anomers of  $C_5OH_9F$  Complexed with Water, Hydrogen Bonding Energies ( $\Delta E_b$  in kcal/mol),<sup>a</sup> Major Structural Parameters (Å), and Delocalization Energies ( $DE^0$  in kcal/mol)

structure	$\Delta E_{\alpha \rightarrow \beta}$			$\Delta E_b$	R(H...O2)	R(H...F)	R(O2-C1)	R(C1-F)	$DE^0$
	MP2	HF	BLW						
$\alpha$ - $C_5OH_9F$							1.3888	1.4237	35.01
$\beta$ - $C_5OH_9F$	3.41	2.79	3.48				1.4054	1.3907	35.70
M1_α				−5.13	1.9043		1.3997	1.4162	34.47
M1_β	2.41	2.10	2.58	−5.96	1.9113		1.4118	1.3913	35.04
M2_α				−4.21		1.9406	1.3782	1.4469	34.90
M2_β	4.12	2.96	2.55	−3.86		2.0354	1.4028	1.4055	35.18
M3_α				−9.10	1.9105	1.9656	1.3897	1.4369	34.29
M3_β	3.08	2.35	1.86	−9.56	1.9040	2.0922	1.4103	1.4050	34.56

<sup>a</sup> $\Delta E_b$  is the energy difference between the complex and the monomers with the basis set superposition error (BSSE) correction at the MP2 level.

electron delocalization, steric interaction and electron correlation. However, both electron delocalization energy and the steric energy can be influenced by the solute–solvent interactions, and thus can be further divided into an intrinsic term and a secondary term due to the solute–solvent interaction. Our analyses show that for anomeric systems, the solute–solvent interaction diminishes the electron delocalization in  $\beta$  anomers more than  $\alpha$  anomers, thus enlarging the anomeric effect in polar solution with reference to the gas phase. In contrast, the solute–solvent interaction significantly reduces the steric energy in  $\beta$  anomers. This can be well understood because of the larger dipole moments of  $\beta$  anomers than those of  $\alpha$  anomers. We also note that both the intrinsic delocalization energy and intrinsic steric energy change little in solutions and are comparable to the values in gas phase. This reinforces the fact that the solute–solvent interaction is responsible for the diminishing of the anomeric effect in solution.

If we combine the intrinsic delocalization energy and intrinsic steric energy together as the internal energy ( $\Delta E_{\text{HF}}^{\text{SO}}$ ), and the secondary energy terms for delocalization and steric effect together as the overall solvation energy ( $\Delta E_{\text{HF}}^{\text{V}}$ ), we observe the different behaviors of  $\Delta E_{\text{HF}}^{\text{SO}}$  and  $\Delta E_{\text{HF}}^{\text{V}}$  in all systems. For anomeric systems that have positive  $\alpha$ – $\beta$  internal energy changes, the solvation energy changes are negative and thus reduce the magnitude of the anomeric effect. But for non- or reverse anomeric systems that have negative  $\alpha$ – $\beta$  internal energy changes, the solvation energy changes are positive. Either way, the solute–solvent interactions tend to reduce the  $\alpha$ – $\beta$  energy gaps.

## COMPUTATIONAL METHODS

Valence bond (VB) theory adopts a bottom-up approach to interpret the molecular structures. It analyzes a molecule using electron-localized resonance states, each of which can be defined by a Heitler–London–Slater–Pauling (HLSP) function.<sup>61–63</sup> Usually a molecule can be well represented with one such state corresponding to the conventional Lewis structure, and any intramolecular electron delocalization (conjugation or hyperconjugation) can be described with the addition of extra (mostly ionic) resonance states. For a resonance structure  $L$  with  $N$  electrons (here we assume closed-shell cases, i.e.,  $N$  is an even number), its HLSP can be expressed as

$$\Psi_L = N_L \hat{A} \{ (\varphi_1 \varphi_2 \varphi_3 \cdots \varphi_N) \prod_{ij} [\alpha(i)\beta(j) - \beta(i)\alpha(j)] \} \quad (1)$$

where  $N_L$  is the normalization constant and  $\hat{A}$  is an antisymmetrizer, and in the above resonance structure  $L$ , two electrons on orbitals  $\varphi_i$  and  $\varphi_j$  form a chemical bond. Apparently, each HLSP can be expanded into  $2^{N/2}$  Slater determinants. Unlike MO theory where all orbitals are delocalized over the whole system with the constraint of mutual orthogonality, VB theory constructs wave functions with localized orbitals without the orbital orthogonality constraint. These localized orbitals can be atomic orbitals as in the classical VB theory, but in modern VB theory, fragmental or functional group orbitals that are variational can be used as localized orbitals.

The fundamental idea of the BLW method is to reduce the number of Slater determinants for a VB function.<sup>59,60</sup> In the BLW method, we partition the molecular system into several blocks (or fragments or groups) and limit the block-localized MOs (BL-MOs) to expand within only one block and doubly occupied in closed-shell cases. In such a way, a HLSP function can be reduced to a BLW as

$$\Psi_{\text{BLW}} = N_L \hat{A} \{ \Omega^1 \Omega^2 \cdots \Omega^K \} \quad (2)$$

where  $\Omega^i$  is a successive product of  $n_i/2$  doubly occupied orbitals in block  $i$ :

$$\Omega^i = \varphi_1^i \alpha \varphi_1^i \beta \cdots \varphi_{n_i/2}^i \alpha \varphi_{n_i/2}^i \beta \quad (3)$$

BL-MOs in the same block are constrained to be orthogonal like in MO methods, but among different blocks they are nonorthogonal like in VB theory. If we allow all orbitals to expand in the whole space of primitive orbitals, the BLW will be upgraded to the familiar Hartree–Fock (HF, or Kohn–Sham within the density functional theory, DFT) wave function  $\Psi_{\text{D}}$ , corresponding to a delocalized state, which is implicitly a superposition of all electron-localized states. Thus, the energy difference between  $\Psi_{\text{BLW}}$  and  $\Psi_{\text{D}}$  is generally defined as the delocalization energy ( $\text{DE}^0$ ),<sup>36</sup> which is a stabilizing force by definition

$$\text{DE}^0 = E(\Psi_{\text{BLW}}) - E(\Psi_{\text{D}}) \quad (4)$$

Although PCM approaches<sup>78,80</sup> do not consider discrete description of solvation or nonequilibrium effects, they have been proven to be an effective and economical way for the investigation of solvation effect within the VB theory.<sup>89</sup> In the PCM method, the solute molecule is treated quantum mechanically, and the interaction between solute and solvent is described as a perturbation on the Hamiltonian of the solute molecule. The total energy of a solvated molecule is

$$\begin{aligned} E^S &= \langle \Psi^S | H^0 + V_R | \Psi^S \rangle \\ &= \langle \Psi^S | H^0 | \Psi^S \rangle + \langle \Psi^S | V_R | \Psi^S \rangle \\ &= E^{\text{SO}} + E^V \end{aligned} \quad (5)$$

where  $H^0$  is the Hamiltonian of the solute molecule in gas phase and  $V_R$  is the solvent reaction potential term, which also depends on the wave function of the solute. In general,  $V_R$  is a sum of the electrostatic, repulsion, and dispersion contributions to the solvent effect. But in practice, only the electrostatic component is related to the solute's wave function, while the rest of the nonelectrostatic components are taken as empirical parameters. Song et al. first incorporated the PCM method into ab initio VB computations where VB wave functions are optimized in the presence of a polarizing field of the solvent self-consistently.<sup>89</sup> Overcoming the disadvantages of inexplicit solvent models, Mo and Gao developed the combined QM(BLW)/MM approach, which considers the solvent molecules explicitly in the derivation of energy profiles of electron-localized states.<sup>90</sup> But here we will focus on the incorporation of the PCM approach into the BLW method, which leads to the energy of the electron-localized state in solution as

$$E_{\text{BLW}}^S = \langle \Psi_{\text{BLW}}^S | H^0 + V_R | \Psi_{\text{BLW}}^S \rangle = E_{\text{BLW}}^{\text{SO}} + E_{\text{BLW}}^V \quad (6)$$

where  $\Psi_{\text{BLW}}^S$  is the block-localized wave function of the solute molecule in solution,  $E_{\text{BLW}}^{\text{SO}}$  accounts for the internal energy of the solute molecule, and  $E_{\text{BLW}}^V$  is the solute–solvent interaction energy calculated with the electron-localized and self-consistent reaction field operator. By extending the expansion of the block-localized orbitals in the whole basis space of the solute molecule, we get the electron-delocalized HF wave function in solution with its energy

$$E_{\text{HF}}^S = \langle \Psi_{\text{HF}}^S | H^0 + V_R | \Psi_{\text{HF}}^S \rangle = E_{\text{HF}}^{\text{SO}} + E_{\text{HF}}^V \quad (7)$$

Similar to eq 4, we can define the delocalization energy in solution as the energy difference between electron-localized and -delocalized wave functions as

$$\begin{aligned} \text{DE}^S &= E_{\text{BLW}}^S - E_{\text{HF}}^S \\ &= (E_{\text{BLW}}^{\text{SO}} - E_{\text{HF}}^{\text{SO}}) + (E_{\text{BLW}}^V - E_{\text{HF}}^V) \\ &= \text{DE}^{\text{SO}} + \text{SE}^V \end{aligned} \quad (8)$$

where  $\text{DE}^{\text{SO}}$  is the intramolecular delocalization energy, which can be regarded as an intrinsic property of the solute, and  $\text{SE}^V$  denotes the secondary electron delocalization effect, or the influence of the solute–solvent interaction on the electron delocalization. The MP2 method considers the electron correlation in a second-order perturbation as the HF energy is the first order energy. Thus, MP2 energy is the summation of the HF energy with an additional electron correlation contribution as

$$E_{\text{MP2}}^{\text{S}} = E_{\text{HF}}^{\text{S}} + E_{\text{c}} \quad (9)$$

Accordingly, the energy difference between  $\alpha$  and  $\beta$  anomers at the MP2 level can be decomposed into three energy terms in two ways as

$$\begin{aligned} \Delta E_{\text{MP2}}^{\text{S}} &= E_{\text{MP2}}^{\text{S}}(\beta) - E_{\text{MP2}}^{\text{S}}(\alpha) \\ &= \Delta E_{\text{HF}}^{\text{S0}} + \Delta E_{\text{HF}}^{\text{V}} + \Delta E_{\text{c}} \\ &= -\Delta E^{\text{S}} + \Delta E_{\text{s}} + \Delta E_{\text{c}} \end{aligned} \quad (10)$$

where  $\Delta E_{\text{s}}$  refers to the intrinsic steric effect ( $\Delta E_{\text{s}}^{\text{S0}}$ )<sup>36,39,40</sup> and the secondary effect due to the solute–solvent interactions ( $\Delta E_{\text{s}}^{\text{V}}$ ) and is expressed as

$$\begin{aligned} \Delta E_{\text{s}} &= E_{\text{BLW}}^{\text{S}}(\beta) - E_{\text{BLW}}^{\text{S}}(\alpha) \\ &= E_{\text{BLW}}^{\text{S0}}(\beta) - E_{\text{BLW}}^{\text{S0}}(\alpha) + E_{\text{BLW}}^{\text{V}}(\beta) - E_{\text{BLW}}^{\text{V}}(\alpha) \\ &= \Delta E_{\text{s}}^{\text{S0}} + \Delta E_{\text{s}}^{\text{V}} \end{aligned} \quad (11)$$

In this work, all optimal geometries of substituted tetrahydropyran  $\text{C}_5\text{OH}_2\text{Y}$  ( $\text{Y} = \text{F}, \text{Cl}, \text{OH}, \text{NH}_2$ , and  $\text{CH}_3$ ) and tetrahydrothiopyran  $\text{C}_5\text{SH}_2\text{Y}$  ( $\text{Y} = \text{F}, \text{Cl}, \text{OH}$ , and  $\text{CH}_3$ ) with vibrational frequency computations were derived at the MP2/6-31+G(d) level with the Gaussian 03 program.<sup>91</sup> The subsequent generalized BLW calculations were performed using the Xiamen Valence Bond (XMVB) program.<sup>92,93</sup> In BLW computations, C1–X, C1–Y, and X–C3  $\sigma$  bonds were localized between the two bonding atoms, while the lone pairs on X and the electrons on group Y were constrained to the respective atom and the functional group. Finally, the remaining 13 doubly occupied BL-MOs were strictly localized on the  $\text{C}_5\text{H}_9$  fragment. The atomic electron population changes due to the electron delocalization interactions and the solvent effect were monitored using the natural population analysis (NPA).<sup>94</sup> All BLW calculations with PCM model were performed using the VBPCM method,<sup>89</sup> which was ported to the quantum mechanical software GAMESS.<sup>95</sup> Frozen cores (1s orbitals) were adopted for all heavy atoms including carbon, nitrogen, oxygen, sulfur, and halogen elements. Note that in all PCM computations, optimal gas-phase geometries are used.

## AUTHOR INFORMATION

### Corresponding Authors

\*E-mail: weiwu@xmu.edu.cn.

\*E-mail: yirong.mo@wmich.edu.

### Notes

The authors declare no competing financial interest.

## ACKNOWLEDGMENTS

This work was supported by the US National Science Foundation under Grants CHE-1055310 and CNS-1126438. C.W. acknowledges the financial support from the China Scholarship Council (CSC). W.W. is grateful for the funding from the National Science Foundation of China (20873106) and the Ministry of Science and Technology of China (2011CB808504).

## REFERENCES

- (1) Edward, J. T. *Chem. Ind. (London, U. K.)* **1955**, 1102.
- (2) Lemieux, R. U.; Chü, P. In *133rd National Meeting of the American Chemical Society*; American Chemical Society: San Francisco, 1958; p 31N.
- (3) Eliel, E. L. *Angew. Chem., Int. Ed.* **1972**, *11*, 739.
- (4) Lemieux, R. U. *Pure Appl. Chem.* **1971**, *25*, 527.
- (5) Wolfe, S.; Rauk, A.; Tel, L. M.; Csizmadia, I. G. *J. Chem. Soc. B* **1971**, 136.
- (6) Reed, A. E.; Schleyer, P. v. R. *J. Am. Chem. Soc.* **1987**, *109*, 7362.
- (7) Salzner, U.; Schleyer, P. v. R. *J. Am. Chem. Soc.* **1993**, *115*, 10231.
- (8) Trapp, M.; Watts, J. K.; Weinberg, N.; Pinto, B. M. *Can. J. Chem.* **2006**, *84*, 692.

- (9) Wolfe, S. *Acc. Chem. Res.* **1972**, *5*, 102.
- (10) Romers, C.; Altona, C.; Buys, H. R.; Havinga, E. *Top. Stereochem.* **1969**, *4*, 39.
- (11) Hillig, K. W., II; Lattimer, R. P.; Kuczkowski, R. L. *J. Am. Chem. Soc.* **1982**, *104*, 988.
- (12) Fuchs, B.; Schleifer, L.; Tartakovsky, E. *New J. Chem.* **1984**, *8*, 275.
- (13) LaBarge, M. S.; Keul, H.; Kuczkowski, R. L.; Wallasch, M.; Cremer, D. *J. Am. Chem. Soc.* **1988**, *110*, 2081.
- (14) Tvaroska, L.; Bleha, T. *Adv. Carbohydr. Chem. Biochem.* **1989**, *47*, 45.
- (15) Narasimhamurthy, N.; Manohar, H.; Samuelson, A. G.; Chandrasekhar, J. *J. Am. Chem. Soc.* **1990**, *112*, 2937.
- (16) Schleifer, L.; Senderowitz, H.; Aped, P.; Tartakovsky, E.; Fuchs, B. *Carbohydr. Res.* **1990**, *206*, 21.
- (17) Suárez, D.; Sordo, T. L.; Sordo, J. A. *J. Am. Chem. Soc.* **1996**, *118*, 9850.
- (18) *Anomeric Effect: Origin and Consequences*; Szarek, W. A.; Horton, D., Eds.; American Chemical Society: Washington, D.C., 1979.
- (19) Kirby, A. J. *Anomeric Effect and Related Stereoelectronic Effects at Oxygen*; Springer-Verlag: Berlin, 1983.
- (20) Deslongchamps, P. *Stereoelectronic Effects in Organic Chemistry*; Elsevier: New York, 1983.
- (21) Krol, M. C.; Huige, C. J. M.; Altona, C. J. *Comput. Chem.* **1990**, *11*, 765.
- (22) Juaristi, E.; Cuevas, G. *Tetrahedron* **1992**, *48*, 5019.
- (23) Salzner, U.; Schleyer, P. v. R. *J. Org. Chem.* **1994**, *59*, 2138.
- (24) *The Anomeric Effect and Associated Stereoelectronic Effects*; Thatcher, G. R., Ed.; American Chemical Society: Washington, D.C., 1993; Vol. 539.
- (25) Juaristi, E.; Cuevas, G. *The Anomeric Effect*; CRC Press: Boca Raton, FL, 1995.
- (26) Omoto, K.; Marusaki, K.; Hirao, H.; Imade, M.; Fujimoto, H. *J. Phys. Chem. A* **2000**, *104*, 6499.
- (27) Weldon, A. J.; Vickrey, T. L.; Tschumper, G. S. *J. Phys. Chem. A* **2005**, *109*, 11073.
- (28) Bitzer, R. S.; Barbosa, A. G. H.; da Silva, C. O.; Nascimento, M. A. C. *Carbohydr. Res.* **2005**, *340*, 2171.
- (29) Boone, M. A.; Striegel, A. M. *Macromolecules* **2006**, *39*, 4128.
- (30) Wiberg, K. B.; Wilson, S. M.; Wang, Y.-G.; Vaccaro, P. H.; Cheeseman, J. R.; Luderer, M. R. *J. Org. Chem.* **2007**, *72*, 6206.
- (31) Woodcock, H. L.; Moran, D.; Pastor, R. W.; MacKerell, A. D.; Brooks, B. R. *Biophys. J.* **2007**, *93*, 1.
- (32) Graczyk, P. P.; Mikołajczyk, M. In *Topics in Stereochemistry*; Eliel, E. L., Wilen, S. H., Eds.; John Wiley & Sons: Hoboken, NJ, 2007; Vol. 21.
- (33) Kesharwani, M. K.; Thiel, W.; Ganguly, B. *J. Phys. Chem. A* **2010**, *114*, 10684.
- (34) Cortés-Guzmán, F.; Hernández-Trujillo, J.; Cuevas, G. *Phys. Chem. Chem. Phys.* **2010**, *12*, 13261.
- (35) Eskandari, K.; Vila, A.; Mosquera, R. A. *J. Phys. Chem. A* **2007**, *111*, 8491.
- (36) Mo, Y. *Nat. Chem.* **2010**, *2*, 666.
- (37) Huang, Y.; Zhong, A.-G.; Yang, Q.; Liu, S. *J. Chem. Phys.* **2011**, *134*, 084103.
- (38) Cocinero, E. J.; Çarçabal, P.; Vaden, T. D.; Simons, J. P.; VDavis, B. G. *Nature* **2011**, *469*, 76.
- (39) Wang, C.; Ying, F.; Wu, W.; Mo, Y. *J. Am. Chem. Soc.* **2011**, *133*, 13731.
- (40) Wang, C.; Chen, Z.; Wu, W.; Mo, Y. *Chem.—Eur. J.* **2013**, *19*, 1436.
- (41) Greenway, K. T.; Bischoff, A. G.; Pinto, B. M. *J. Org. Chem.* **2012**, *77*, 9221.
- (42) Alabugin, I. V. *J. Org. Chem.* **2000**, *65*, 3910.
- (43) Pinto, B. M.; Schlegel, H. B.; Wolfe, S. *Can. J. Chem.* **1987**, *65*, 1658.
- (44) Fuchs, B.; Ellencweig, A.; Tartakovsky, E.; Aped, P. *Angew. Chem., Int. Ed.* **1986**, *25*, 287.



- (45) Wolfe, S.; Pinto, B. M.; Varma, V.; Leung, R. Y. N. *Can. J. Chem.* **1990**, *68*, 1051.
- (46) Schelyer, P. v. R.; Kos, A. J. *Tetrahedron* **1983**, *39*, 1141.
- (47) Anderson, C. B.; Sepp, D. T. *J. Org. Chem.* **1967**, *32*, 607.
- (48) Perrin, C. L.; Armstrong, K. B.; Fabian, M. A. *J. Am. Chem. Soc.* **1994**, *116*, 715.
- (49) Lemieux, R. U.; Pavia, A. A.; Martin, J. C.; Wantanabe, K. A. *Can. J. Chem.* **1969**, *47*, 4427.
- (50) Praly, J.-P.; Lemieux, R. U. *Can. J. Chem.* **1987**, *65*, 213.
- (51) Cramer, C. J. *J. Org. Chem.* **1992**, *57*, 7034.
- (52) Ha, S. H.; Gao, J.; Tidor, B.; Brady, J. W.; Karplus, M. *J. Am. Chem. Soc.* **1991**, *113*, 1553.
- (53) Box, V. G. S. *Heterocycles* **1990**, *31*, 1157.
- (54) Box, V. G. S. *Heterocycles* **1998**, *48*, 2389.
- (55) Box, V. G. S. *J. Mol. Struct.* **2000**, *522*, 145.
- (56) Favero, L. B.; Caminati, W.; Velino, B. *Phys. Chem. Chem. Phys.* **2003**, *5*, 4776.
- (57) Vila, A.; Mosquera, R. A. *J. Comput. Chem.* **2007**, *28*, 1516.
- (58) Takahashia, O.; Yamasakia, K.; Kohnob, Y.; Ohtakib, R.; Uedab, K.; Suezawac, H.; Umezawad, Y.; Nishioe, M. *Carbohydr. Res.* **2007**, *342*, 1202.
- (59) Mo, Y.; Peyerimhoff, S. D. *J. Chem. Phys.* **1998**, *109*, 1687.
- (60) Mo, Y.; Song, L.; Lin, Y. J. *Phys. Chem. A* **2007**, *111*, 8291.
- (61) *Valence Bond Theory*; Cooper, D. L., Ed.; Elsevier: Amsterdam, **2002**.
- (62) Gallup, G. A. *Valence Bond Methods: Theory and Applications*; Cambridge University Press: New York, **2002**.
- (63) Shaik, S. S.; Hiberty, P. C. *A Chemist's Guide to Valence Bond Theory*; Wiley: Hoboken, NJ, **2008**.
- (64) Bader, R. F. W. *Atoms in Molecules: A Quantum Theory*; Oxford University Press: Oxford, U.K., **1990**.
- (65) Reed, A. E.; Curtiss, L. A.; Weinhold, F. *Chem. Rev.* **1988**, *88*, 899.
- (66) Weinhold, F.; Landis, C. *Valency and Bonding*; Cambridge University Press: New York, **2005**.
- (67) Stoll, H.; Preuss, H. *Theor. Chim. Acta* **1977**, *46*, 11.
- (68) Stoll, H.; Wagenblast, G.; Preuss, H. *Theor. Chim. Acta* **1980**, *57*, 169.
- (69) Mehler, E. L. *J. Chem. Phys.* **1977**, *67*, 2728.
- (70) Mehler, E. L. *J. Chem. Phys.* **1981**, *74*, 6298.
- (71) Gianinetti, E.; Raimondi, M.; Tornaghi, E. *Int. J. Quantum Chem.* **1996**, *60*, 157.
- (72) Famulari, A.; Gianinetti, E.; Raimondi, M.; Sironi, M. *Int. J. Quantum Chem.* **1998**, *69*, 151.
- (73) Khaliullin, R. Z.; Cobar, E. A.; Lochan, R. C.; Bell, A. T.; Head-Gordon, M. *J. Phys. Chem. A* **2007**, *111*, 8753.
- (74) Angyal, S. J. *Angew. Chem., Int. Ed.* **1969**, *8*, 157.
- (75) Kotowycz, G.; Lemieux, R. U. *Chem. Rev.* **1973**, *73*, 669.
- (76) Franks, F. *Pure Appl. Chem.* **1987**, *59*, 1189.
- (77) Juaristi, E.; Tapia, J.; Mendez, R. *Tetrahedron* **1986**, *42*, 1253.
- (78) Miertuš, S.; Scrocco, E.; Tomasi, J. *Chem. Phys.* **1981**, *55*, 117.
- (79) Spiwok, V.; French, A. D. *Mini-Rev. Org. Chem.* **2011**, *8*, 249.
- (80) Tomasi, J.; Mennucci, B.; Cammi, R. *Chem. Rev.* **2005**, *105*, 2999.
- (81) Carballeira, L.; Pérez-Juste, I. *J. Comput. Chem.* **2000**, *21*, 462.
- (82) Carballeira, L.; Pérez-Juste, I. *J. Comput. Chem.* **2001**, *22*, 135.
- (83) Vila, A.; Estevez, L.; Mosquera, R. A. *J. Phys. Chem. A* **2011**, *115*, 1964.
- (84) Mo, Y.; Gao, J. *Acc. Chem. Res.* **2007**, *40*, 113.
- (85) Lemieux, R. U.; Morgan, A. R. *Can. J. Chem.* **1965**, *43*, 2205.
- (86) Fabian, M. A.; Perrin, C. L.; Sinnott, M. L. *J. Am. Chem. Soc.* **1994**, *116*, 8398.
- (87) Perrin, C. L.; Fabian, M. A.; Brunckova, J.; Ohta, B. K. *J. Am. Chem. Soc.* **1999**, *121*, 6911.
- (88) Perrin, C. L.; Armstrong, K. B. *J. Am. Chem. Soc.* **1993**, *115*, 6825.
- (89) Song, L.; Wu, W.; Zhang, Q.; Shaik, S. J. *Phys. Chem. A* **2004**, *108*, 6017.
- (90) Mo, Y.; Gao, J. *J. Phys. Chem. A* **2000**, *104*, 3012.
- (91) Frisch, M. J.; Trucks, G. W.; Schlegel, H. B.; Scuseria, G. E.; Robb, M. A.; Cheeseman, J. R.; Montgomery, J. A., Jr.; Vreven, T.; Kudin, K. N.; Burant, J. C.; Millam, J. M.; Iyengar, S. S.; Tomasi, J.; Barone, V.; Mennucci, B.; Cossi, M.; Scalmani, G.; Rega, N.; Petersson, G. A.; Nakatsuji, H.; Hada, M.; Ehara, M.; Toyota, K.; Fukuda, R.; Hasegawa, J.; Ishida, M.; Nakajima, T.; Honda, Y.; Kitao, O.; Nakai, H.; Klene, M.; Li, X.; Knox, J.; Hratchian, H. P.; Cross, J. B.; Bakken, V.; Adamo, C.; Jaramillo, J.; Gomperts, R.; Stratmann, R. E.; Yazyev, O. A.; Austin, J.; Cammi, R.; Pomelli, C.; Ochterski, J. W.; Ayala, P. Y.; Morokuma, K.; Voth, G. A.; Salvador, P.; Dannenberg, J. J.; Zakrzewski, V. G.; Dapprich, S.; Daniels, A. D.; Strain, M. C.; Farkas, O.; Malick, D. K.; Rabuck, A. D.; Raghavachari, K.; Foresman, J. B.; Ortiz, J. V.; Cui, Q.; Baboul, A. G.; Clifford, S.; Cioslowski, J.; Stefanov, B. B.; Liu, G.; Liashenko, A.; Piskorz, P.; Komaromi, I.; Martin, R. L.; Fox, D. J.; Keith, T.; Al-Laham, M. A.; Peng, C. Y.; Nanayakkara, A.; Challacombe, M.; Gill, P. M. W.; Johnson, B.; Chen, W.; Wong, M. W.; Gonzalez, C.; Pople, J. A. *Gaussian 03*, E.01; Gaussian, Inc.: Wallingford, CT, **2004**.
- (92) Song, L.; Song, J.; Mo, Y.; Wu, W. *J. Comput. Chem.* **2009**, *30*, 399.
- (93) Song, L.; Chen, Z.; Ying, F.; Song, J.; Chen, X.; Su, P.; Mo, Y.; Zhang, Q.; Wu, W. *Xiamen Valence Bond*; Xiamen University: Xiamen, China, **2012**.
- (94) Reed, A. E.; Weinstock, R. B.; Weinhold, F. *J. Chem. Phys.* **1985**, *83*, 735.
- (95) Schmidt, M. W.; Baldridge, K. K.; Boatz, J. A.; Elbert, S. T.; Gordon, M. S.; Jensen, J. J.; Koseki, S.; Matsunaga, N.; Nguyen, K. A.; Su, S.; Windus, T. L.; Dupuis, M.; Montgomery, J. A. *J. Comput. Chem.* **1993**, *14*, 1347.